Conformationally-locked metallomacrocycles—prototypes for a novel type of axial chirality†‡

Hoi Shan Chow,[a] Edwin C. Constable,*[a] Richard Frantz,[b] Catherine E. Housecroft,[a] Jérôme Lacour,*[b] Markus Neuburger,[a] Dmitrij Rappoport[c] and Silvia Schaffner[a]

Received (in Montpellier, France) 4th November 2008, Accepted 5th December 2008
First published as an Advance Article on the web 8th January 2009
DOI: 10.1039/b819588a

A series of ditopic ligands incorporating two 2,2′:6′,2″-terpyridine (tpy) metal-binding domains linked to a central naphthalenediyl core by ethyleneoxy chains of various lengths have been prepared and their iron(II) complexes prepared. The major thermodynamic products of complexation are ferracycles of [1 + 1], [2 + 2] or [3 + 3] stoichiometry. In the case of the [1 + 1] complexes, the linker between the two tpy domains is spatially restricted and the cations exhibit chirality associated with the conformation about the central N–Fe–N bonds. The dynamic processes by which the enantiomeric forms interconvert are investigated in the presence of chiral anions by NMR and circular dichroism spectroscopy making use of the Pfeiffer effect. We have shown that ditopic bis(2,2′:6′,2″-terpyridine) ligands give rise to conformationally restricted complexes with iron(II) centres. The absolute configuration of the cations in the diastereomeric ion pairs obtained through the Pfeiffer effect has been calculated using TDDFT methods.

Introduction

Chirality has played an important role in inorganic chemistry since the pioneering stereochemical investigations in coordination chemistry by Alfred Werner.[1] There is a number of common manifestations of chirality in coordination chemistry, the most common of which arise when chiral ligands or counter-ions are utilized or when bidentate ligands LL are involved in complexes of the type $[M(LL)_3]^{n+}$ or *cis*-$[M(LL)_2X_2]^{n+}$ (X = monodentate ligand) as indicated in Scheme 1.[2] The classic examples of chiral complexes involving bidentate ligands utilize derivatives of 1,2-diaminoethane (en), 2,2′-bipyridine (bpy) or 1,10-phenanthroline (phen).[3] The latter ligands are the parent members of a class of oligopyridine ligands of which the next higher member is typified by 2,2′:6′,2″-terpyridine (tpy).[4–7] Although both $[M(bpy)_3]^{n+}$ and $[M(tpy)_2]^{n+}$ motifs present N_6 donor sets to the metal, the former with D_3 symmetry exists as the pair of Δ and Λ enantiomers, whilst the latter with D_{2d} symmetry is achiral. In the case of substituted bpy and tpy ligands other stereochemical complexities arise. In particular, in the case of asymmetric tpy ligands substituted on the terminal rings the symmetry of $[ML_2]^{n+}$ complexes is lowered to C_2 and a pair of Δ and Λ enantiomers are formed.[2] We have recently been interested in ditopic ligands 4′-tpy-S-tpy-4′ in which two

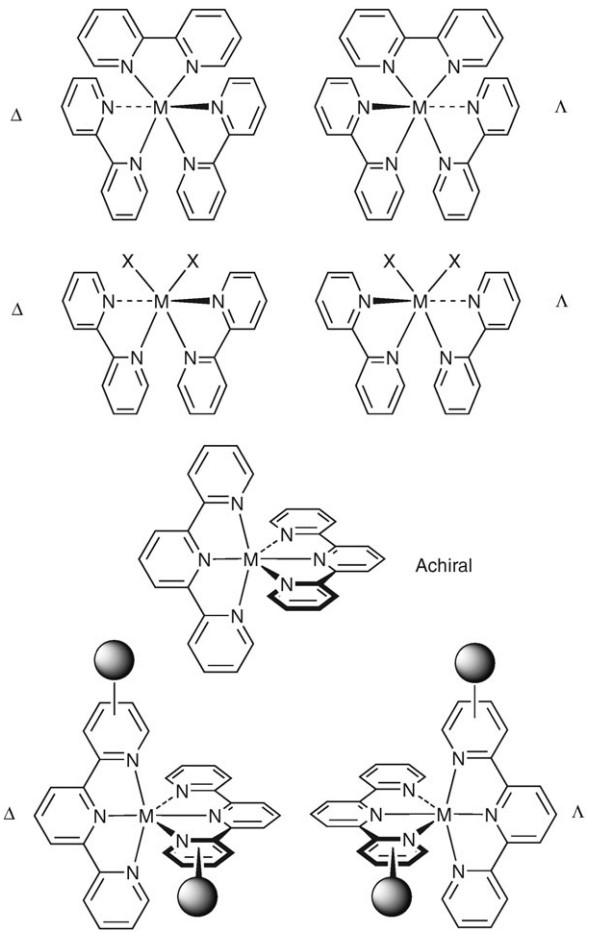

Scheme 1 Stereochemical relationships in six-coordinated complexes of chelating ligands. The stereochemical descriptors Δ and Λ are used to describe the absolute configuration of the chiral complexes obtained with asymmetrically-substituted tpy ligands. The skew line convention adopted assigns the substituted ring of the terpy the highest priority.

[a] *Department of Chemistry, University of Basel, Spitalstrasse 51, CH4056 Switzerland. E-mail: edwin.constable@unibas.ch; Fax: +41 (0)61 267 1018; Tel: +41 (0)61 267 1001*
[b] *Department of Organic Chemistry, University of Geneva, Quai E. Ansermet 30, CH-1211 Geneva 4 Switzerland. E-mail: jerome.lacour@unige.ch; Fax: +41 (0)22 379 6526*
[c] *Department of Chemistry, University of California Irvine, Irvine, CA 92697, USA*

† Dedicated to Prof. Jean-Pierre Sauvage on the occasion of his 65th birthday.

‡ CCDC reference number 712233. For crystallographic data in CIF or other electronic format see DOI: 10.1039/b819588a

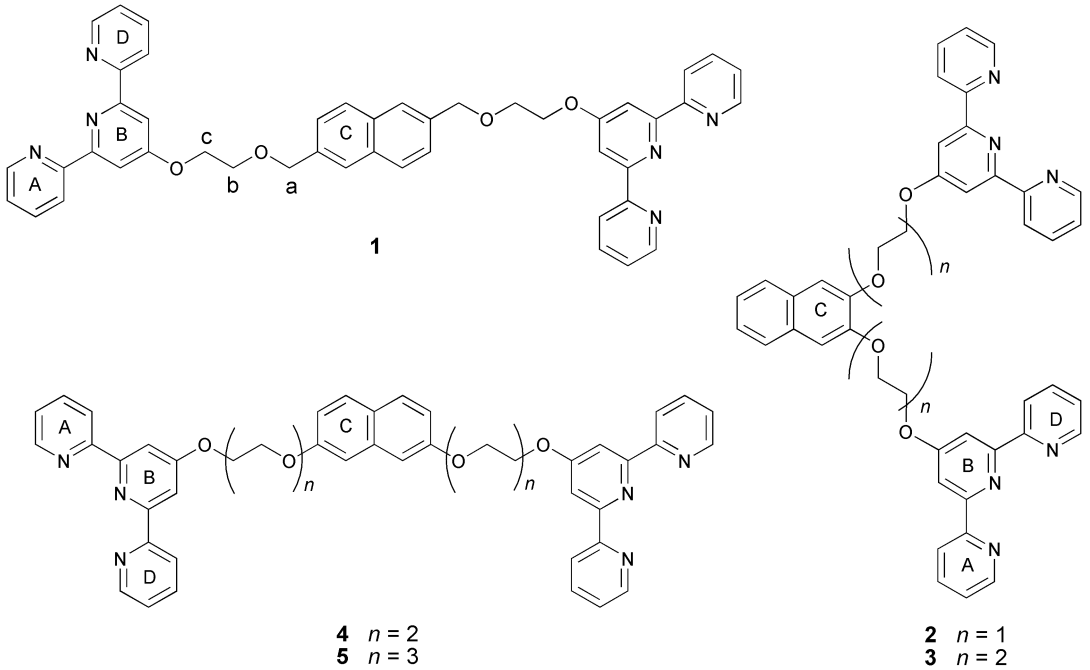

Scheme 2 Structures of ligands **1–5** with ring labelling for NMR spectroscopic assignments.

4′-substituted tpy metal-binding domains are linked by a variety of spacer groups S. These species can variously give rise to metallopolymers or metallocycles and we have shown that the thermodynamic products are, as expected, the metallomacrocycles.[8–12] We have also shown that complexes of these ligands are activated towards nucleophilic attack at the 4′-position with the eventual conversion of the ditopic ligand into two "simple" tpy metal-binding domains.[13] In the course of this work we encountered a mononuclear metallocyclic complex $[Fe(\mathbf{4})]^{2+}$ (see Scheme 2 for ligand **4**) in which the restricted rotation on the NMR time scale of the spacer resulted in the formation of chiral complexes,[9] a phenomenon that could be viewed as a form of atropisomerism.[14] In this paper we report further studies on this phenomenon and present further examples demonstrating the role of the spacer.

Experimental

General

Infrared spectra were recorded on Shimadzu FTIR 8300 or FTIR-8400S Fourier-transform spectrophotometers with samples as solids using a Golden Gate ATR accessory. ^{1}H and ^{13}C NMR spectra were recorded on Bruker DRX 500 MHz and ARX-500 spectrometers at room temperature; the ring labelling used for the ligands is shown in Scheme 2; chemical shifts are referenced with respect to residual solvent peaks and TMS = δ 0 ppm. FAB and electrospray (ES) mass spectra were recorded on Finnigan MAT95Q and MAT LCQ instruments; FAB MS used 3-nitrobenzyl alcohol as supporting matrix. Electronic absorption spectra were recorded on a Shimadzu UV-3101PC spectrophotometer. Circular dichroism spectra were recorded on a JASCO J-715 polarimeter in a 1.0 cm quartz cell; λ are given in nm. Reactions were carried out under nitrogen. All solvents were dried and distilled before use. 4′-Chloro-2,2′:6′,2″-terpyridine,[15] ligands **1–4**[12] and the chiral anions TRISPHAT (tris(tetrachlorobenzenediolato)-phosphate(v)),[16] BINPHAT (bis(tetrachlorobenzenediolato)-mono([1,1′]-binaphthalenyl-2,2′-diolato)phosphate(v))[17] and SUGARPHAT (bis(tetrachlorobenzenediolato)[(6*S*,7*S*,8*R*)-6-methoxy-2,2-dimethylhexahydropyrano[3,2-d][1,3]dioxine-7,8-diolato]phosphate(v)[18,19] were prepared as previously reported.

Syntheses

2,7-Di{2-[2-(2-hydroxyethoxy)ethoxy]ethoxy}naphthalene. 2,7-Dihydroxynaphthalene (1.6 g, 10 mmol), K_2CO_3 (12 g, 90 mmol) were stirred in acetone (150 mL) for 2 h at 70 °C. Then, 2-[2-(2-chloroethoxy)ethoxy]ethanol (5.06 g, 30 mmol) was added dropwise to the reaction mixture and stirring was continued for 3 days with the temperature maintained at 70 °C. A spot TLC indicated that the reaction was incomplete and so additional 2-[2-(2-chloroethoxy)ethoxy]ethanol (1.68 g, 10 mmol) was added and heating (70 °C) was continued for 2 days. After cooling the mixture to room temperature, solvent was removed under reduced pressure, and the residue was partitioned between CH_2Cl_2 and water (250 mL). The organic layer was separated, dried ($MgSO_4$), and filtered. 2,7-Di{2-[2-(2-hydroxyethoxy)ethoxy]ethoxy}naphthalene was isolated as a black oil (3.5 g, 8.2 mmol, 82%). ^{1}H NMR (500 MHz, $CDCl_3$) δ/ppm 2.76 (br, 2H, H^{OH}), 3.60 (m, 4H, H^{e}), 3.71 (m, 12H, $H^{c,d,f}$), 3.89 (m, 4H, H^{b}), 4.22 (m, 4H, H^{a}), 7.01 (m, 4H, $H^{C1,C3}$), 7.62 (d, J 8.8 Hz, 2H, H^{C4}); ^{13}C NMR (125 MHz, $CDCl_3$) δ/ppm 61.8 (C^{f}), 67.4 (C^{a}), 69.8 (C^{b}), 70.4 (C^{d}), 70.9 (C^{c}), 72.6 (C^{e}), 106.3 (C^{C1}), 116.5 (C^{C3}), 124.6 (C^{C4a}), 129.2 (C^{C4}), 135.8 (C^{C8a}), 157.3 (C^{C2}); FAB-MS m/z 425 $[M]^{+}$; IR (solid, cm^{-1}) 3418br, 2916m, 2870m, 1628s, 1512m, 1458m, 1358w, 1258m, 1211s, 1119s, 1065s, 957w,

887w, 833w. Anal. calcd for $C_{22}H_{32}O_8 \cdot 1/3H_2O$: C, 61.37; H, 7.66. Found: C, 61.46; H, 7.57%.

2,7-[Bis(2,2′ : 6′,2″-terpyridin-4′-yl)-1,4,7,10-tetraoxadecyl]-naphthalene (5). 2,7-Di{2-[2-(2-hydroxyethoxy)ethoxy]ethoxy}-naphthalene (0.70 g, 1.6 mmol) was added to a suspension of finely powdered KOH (1.1 g, 20 mmol) in DMSO (15 mL). The mixture was heated to 70 °C and was stirred at this temperature for 1 h. Then Cltpy (1.3 g, 4.9 mmol) was added and the reaction mixture was stirred at 70 °C for 5 days. After cooling to room temperature, water (500 mL) was added and a white precipitate formed. This was separated by filtration, washed with plenty of water, and dried. The crude product was purified by column chromatography (alumina, CH_2Cl_2–5% CH_3OH) and was collected as the first fraction. Compound **5** was isolated as a pale yellow oil (0.20 g, 0.23 mmol, 14%). ^{1}H NMR (500 MHz, $CDCl_3$) δ/ppm 3.78 (m, 8H, $H^{c,d}$), 3.91 (t, J 4.8 Hz, 4H, H^b), 3.93 (t, J 4.7 Hz, 4H, H^e), 4.19 (t, J 4.9 Hz, 4H, H^a), 4.39 (t, J 4.7 Hz, 4H, H^f), 6.98 (m, 4H, $H^{C1,C3}$), 7.31 (ddd J 7.5, 4.8, 1.2 Hz, 4H, H^{A5}), 7.58 (d, J 9.6 Hz, 2H, H^{C4}), 7.83 (dt J 1.8, 7.7 Hz, 4H, H^{A4}), 8.04 (s, 4H, H^{B3}), 8.59 (td, J 7.9, 1.0 Hz, 4H, H^{A3}), 8.66 (ddd J 4.8, 1.8, 0.9 Hz, 4H, H^{A6}); δ/ppm 67.4 (C^a), 67.9 (C^f), 69.6 (C^e), 69.9 (C^b), 71.0 (C^c), 71.2 (C^d), 106.3 (C^{C1}), 107.6 (C^{B3}), 116.5 (C^{C3}), 121.5 (C^{A3}), 124.0 (C^{A5}), 124.5 (C^{C4a}), 129.1 (C^{C4}), 135.8 (C^{C8a}), 137.0 (C^{A4}), 149.0 (C^{A6}), 156.0 (C^{A2}), 157.1 (C^{B2}), 157.4 (C^{C2}), 167.1 (C^{B4}); FAB-MS m/z 887 $[M]^+$, 250 $[tpyOH]^+$, 221 $[tpy]^+$; IR (solid, cm^{-1}) 3055w, 2870w, 1628m, 1582s, 1558s, 1512m, 1466m, 1443s, 1404s, 1350m, 1257m, 1204s, 1126s, 1056s, 995w, 964w, 872w, 833w, 795m, 733m, 702w. Anal. calcd for $C_{52}H_{50}N_6O_8 \cdot H_2O$: C, 69.01; H, 5.79; N, 9.29. Found: C, 69.15; H, 5.61; N, 9.28%.

$[Fe_2(\mathbf{1})_2][PF_6]_4$. $FeCl_2 \cdot 4H_2O$ (40 mg, 0.20 mmol) was dissolved in CH_3OH (20 mL) and the solution was added dropwise to a solution of **1** (150 mg, 0.20 mmol) in CH_3OH (750 mL). The reaction mixture was stirred at room temperature for 4 days. The crude product was precipitated by addition of aqueous $[NH_4][PF_6]$ and was purified by column chromatography (SiO_2, CH_3CN–saturated aqueous KNO_3–H_2O 14 : 2 : 1). $[Fe_2(\mathbf{1})_2][PF_6]_4$ eluted as a purple (major) fraction. Additional aqueous $[NH_4][PF_6]$ was added to the fraction and $[Fe(\mathbf{1})][PF_6]_2$ was isolated as a purple powder (62 mg, 0.029 mmol, 29%). ^{1}H NMR (500 MHz, CD_3CN) δ/ppm 4.05 (m, 8H, H^b), 4.78 (s, 8H, H^a), 4.81 (m, 8H, H^c), 6.87 (ddd, J 1.3, 5.7, 7.4 Hz, 8H, H^{A5}), 6.99 (ddd, J 0.7, 1.4, 5.6 Hz, 8H, H^{A6}), 7.34 (1.3, 8.4 Hz, 4H, H^{C3}), 7.47 (d, J 8.3 Hz, 4H, H^{C4}), 7.71 (m, 8H, H^{A4}), 7.72 (s, 4H, H^{C1}), 8.29 (td, J 0.9, 8.0 Hz, 8H, H^{A3}), 8.47 (s, 8H, H^{B3}); ES MS m/z 578 $[M - 3PF_6]^{3+}$, 398 $[M - 4PF_6]^{4+}$; UV-Vis (CH_3CN): λ_{max}/nm (λ_{max}, $dm^3\ mol^{-1}\ cm^{-1}$) 226 (145 000), 241 (64 800), 270 (64 300), 314 (38 200), 552 (12 200). Anal. calcd for $C_{92}H_{76}F_{24}Fe_2N_{12}O_8P_4 \cdot 7H_2O$: C, 48.14; H, 3.96; N, 7.32. Found: C, 47.89; H, 3.63; N, 7.47%.

$[Fe_3(\mathbf{2})_3][PF_6]_6$. Preparation and purification were as for $[Fe_2(\mathbf{1})_2][PF_6]_4$ starting with $FeCl_2 \cdot 4H_2O$ (40 mg, 0.20 mmol) and **2** (140 mg, 0.20 mmol) with a reaction time of 4 days. One major band was observed on the chromatography column and most material (intractable) remained on the base line. $[Fe_3(\mathbf{2})_3][PF_6]_6$ was isolated as a purple powder (81 mg, 0.026 mmol, 38%). ^{1}H NMR (500 MHz, CD_3CN) δ/ppm 4.84 (m, 12H, H^a), 5.06 (m, 12H, H^a), 6.87 (t, J 6.5 Hz, 12H, H^{A5}), 7.12 (d, J 5.8 Hz, 12H, H^{A6}), 7.46 (m, 6H, H^{C6}), 7.59 (s, 6H, H^{C1}), 7.60 (m, 12H, H^{A4}), 7.88 (m, 6H, H^{C5}), 8.35 (d, J 8.0 Hz, 12H, H^{A3}), 8.54 (s, 12H, H^{B3}); ES MS m/z 911 $[M - 3PF_6]^{3+}$, 648 $[M - 4PF_6]^{4+}$, 489 $[M - 5PF_6]^{5+}$, 383 $[M - 6PF_6]^{6+}$; UV-Vis (CH_3CN): λ_{max}/nm (λ_{max}, $dm^3\ mol^{-1}\ cm^{-1}$) 230 (143 000), 270 (103 000), 315 (84 200), 560 (40 400). Anal. calcd for $C_{132}H_{102}F_{36}Fe_3N_{18}O_{12}P_6 \cdot 2KPF_6 \cdot 6H_2O$: C, 43.86; H, 3.18; N, 6.97. Found: C, 43.79; H, 3.41; N, 6.87%.

$[Fe_2(\mathbf{3})_2][PF_6]_4$. Preparation and purification were as for $[Fe_2(\mathbf{1})_2][PF_6]_4$ starting with $FeCl_2 \cdot 4H_2O$ (40 mg, 0.20 mmol) and **3** (160 mg, 0.20 mmol) with a reaction time of 4 days. One major band eluted on the chromatography column and most material remained as an intractable solid on the base line. $[Fe_2(\mathbf{3})_2][PF_6]_4$ was isolated as a purple powder (75 mg, 0.033 mmol, 33%). ^{1}H NMR (500 MHz, CD_3CN) δ/ppm 4.14 (m, 8H, H^b), 4.21 (m, 8H, H^c), 4.42 (m, 8H, H^a), 4.79 (m, 8H, H^d), 6.65 (m, 8H, H^{A5}), 6.98 (dd, J 0.6, 5.6 Hz, 8H, H^{A6}), 7.29 (m, 4H, H^{C6}), 7.33 (m, 8H, H^{A4}),7.35 (s, 4H, H^{C1}), 7.67 (m, 4H, H^{C5}), 8.19 (d, J 8.0 Hz, 8H, H^{A3}), 8.41 (s, 8H, H^{B3}); ES MS m/z 618 $[M - 3PF_6]^{3+}$, 427 $[M - 4PF_6]^{4+}$; UV-Vis (CH_3CN): λ_{max}/nm (λ_{max}, $dm^3\ mol^{-1}\ cm^{-1}$) 231 (111 000), 269 (57 900), 314 (40 700), 553 (12 000). Anal. calcd for $C_{96}H_{84}F_{24}Fe_2N_{12}O_{12}P_4 \cdot 2KPF_6 \cdot 6H_2O$: C, 41.69; H, 3.51; N, 6.08. Found: C, 41.55; H, 3.42; N, 6.14%.

$[Fe(\mathbf{4})][PF_6]_2$. Preparation and purification were as for $[Fe(\mathbf{1})][PF_6]_2$ starting with $FeCl_2 \cdot 4H_2O$ (19 mg, 0.096 mmol) and **4** (75 mg, 0.091 mmol) with a reaction time of 2 days. One major band eluted on the chromatography column and most material stayed as an intractable solid on the base line. $[Fe(\mathbf{4})][PF_6]_2$ was isolated as a purple powder (40 mg, 0.035 mmol, 39%). ^{1}H NMR (500 MHz, CD_3CN) δ/ppm 3.79 (m, 6H, $H^{a1,a2,b2}$), 4.07 (m, 2H, H^{b1}), 4.13 (m, 4H, $H^{c1,c2}$), 4.66 (td, J 2.0, 13.9 Hz, 2H, H^{d2}), 4.86 (d, J 2.4 Hz, 2H, H^{C1}), 5.38 (m, 2H, H^{d1}), 6.52 (ddd, J 1.3, 5.7, 7.5 Hz, 2H, H^{A5}), 6.65 (ddd, J 0.7, 1.4, 5.6 Hz, 2H, H^{A6}), 6.85 (dd, J 2.5, 8.9 Hz, 2H, H^{C3}), 7.02 (ddd, J 1.3, 5.6, 7.5 Hz, 2H, H^{D5}), 7.31 (dt, J 1.5, 7.8 Hz, 2H, H^{A4}), 7.35 (ddd, J 0.7, 1.4, 5.6 Hz, 2H, H^{D6}), 7.53 (d, J 9.0 Hz, 2H, H^{C4}). 7.84 (dt, J 1.5, 7.8 Hz, 2H, H^{D4}), 8.18 (d, J 7.8 Hz, 2H, H^{A3}), 8.37 (td, J 1.0, 8.0 Hz, 2H, H^{D3}), 8.41 (d, J 2.2 Hz, 2H, H^{B5}), 8.82 (d, J 2.2 Hz, 2H, H^{B3}); ^{13}C NMR (125 MHz, CD_3CN) δ/ppm 168.6 (C^{B4}), 160.1 ($C^{A2,D2}$), 160.0 ($C^{D2,A2}$), 158.0 ($C^{B2,B6}$), 157.9 ($C^{B6,B2}$), 157.1 ($C^{C4a/8a}$), 153.8 (C^{D6}), 152.0 (C^{A6}), 138.5 (C^{D4}), 138.1 (C^{A4}), 134.8 ($C^{C4a/8a}$), 129.2 (C^{C4}), 126.9 (C^{D5}), 126.4 (C^{A5}), 124.2 (C^{C2}), 123.3 (C^{D3}), 122.7 (C^{A3}), 114.8 (C^{C3}), 114.1 (C^{B5}), 111.0 (C^{B3}), 105.4 (C^{C1}), 72.0 (C^c), 69.4 (C^b), 68.4 (C^d), 67.8 (C^a); ES MS m/z 999 $[M - PF_6]^+$; UV-Vis (CH_3CN): λ_{max}/nm (λ_{max}, $dm^3\ mol^{-1}\ cm^{-1}$) 233 (80 000), 269 (40 700), 314 (31 300), 555 (9300). Anal. calcd for $C_{48}H_{42}F_{12}FeN_6O_6P_2$: C, 50.36; H, 3.71; N, 7.34. Found: C, 50.10; H, 3.71; N, 7.51%.

$[Fe(\mathbf{5})][PF_6]_2$. The methods of preparation and purification were as for $[Fe(\mathbf{1})][PF_6]_2$ starting with $FeCl_2 \cdot 4H_2O$ (32 mg, 0.16 mmol) and **5** (140 mg, 0.16 mmol) with a reaction time of 3 days. One major band was observed on the chromatography

column and most material (intractable) remained on the base line. [Fe(**5**)][PF_6]$_2$ was isolated as a purple powder (94 mg, 0.076 mmol, 48%). ^{1}H NMR (500 MHz, CD_3CN) δ/ppm 3.56 (t, J 4.7 Hz, 4H, H^a), 3.76 (m, 4H, H^c), 3.82 (m, 4H, H^b), 3.86 (m, 4H, H^d), 4.12 (m, 4H, H^e), 4.84 (m, 4H, H^f), 5.44 (d, J 2.4 Hz, 2H, H^{C1}), 6.87 (m, 6H, $H^{A5,C3}$), 7.07 (ddd, J 0.7, 1.3, 5.6 Hz, 4H, H^{A6}), 7.59 (d, J 9.0 Hz, 4H, H^{C4}), 7.60 (dt, J 1.5, 7.8 Hz, 4H, H^{A4}), 8.23 (td, J 0.9, 7.8 Hz, 4H, H^{A3}), 8.51 (s, 4H, H^{B3}); ^{13}C NMR (125 MHz, CD_3CN) δ/ppm 169.5 (C^{B4}), 161.7 (C^{A2}), 159.0 (C^{B2}), 158.3 ($C^{C4a/8a}$), 154.2 (C^{A6}), 139.4 (C^{A4}), 136.5 ($C^{C4a/8a}$), 130.4 (C^{C4}), 128.1 (C^{A5}), 125.3 (C^{C2}), 124.4 (C^{A3}), 116.8 (C^{C3}), 113.0 (C^{B3}), 105.9 (C^{C1}), 71.8 (C^d), 71.7 (C^c), 71.3 (C^f), 70.9 (C^e), 70.3 (C^b), 68.5 (C^a); ES MS m/z 1087 $[M - PF_6]^+$, 471 $[M - 2PF_6]^{2+}$; UV-Vis (CH_3CN): λ_{max}/nm (λ_{max}, dm^3 mol^{-1} cm^{-1}) 232 (170 000), 269 (87 400), 313 (68 900), 554 (20 300). Anal. calcd for $C_{52}H_{50}F_{12}FeN_6O_8P_2$: C, 50.66; H, 4.09; N, 6.82. Found: C, 51.47; H, 4.24; N, 6.47%.

Crystal data for [Fe(5)][PF_6]$_2$·CH_3CN

Data were collected on a Bruker-Nonius Kappa CCD instrument; data reduction, solution and refinement used the programmes COLLECT,[20] SIR92,[21] DENZO/SCALEPACK[22] and CRYSTALS.[23] ORTEP figures were drawn using Ortep-3 for Windows.[24] Crystal data: $C_{54}H_{53}F_{12}FeN_7O_8P_2$, M = 1273.83, purple block, monoclinic, space group $P2_1/c$, a = 18.2659(1), b = 14.8059(1), c = 20.5792(2) Å, β = 92.9257(5), U = 5558.25(7) Å^3, Z = 4, D_c = 1.522 Mg m^{-3}, μ(Mo-K$_\alpha$) = 0.430 mm^{-1}, T = 173 K. Number of reflections measured 54 042 (unique 14324); 8366 observed reflections, $I > 3\sigma(I)$, were used for the determination (811 parameters); the refinement converged at R = 0.0690 (all data), 0.0425 (observed $I > 3\sigma(I)$), wR = 0.0660 (all data), 0.0574 (observed $I > 3\sigma(I)$), min and max residual electron density 0.59 and −0.46 e Å^{-3}; R_{int} = 0.048, gof = 1.12.

Preparation of diastereomeric ion pairs involving $[Fe(4)]^{2+}$. Ion exchange metathesis

To a solution of salt [Fe(**4**)][PF_6]$_2$ (1.0 equiv.) in CH_2Cl_2 (2.5 mL) were added solutions of [cinchonidinium][Δ-**6**], [Me_2NH_2][Λ-**7**] or [Me_2NH_2][Δ-**8**] (2.5 equiv.) in acetone (2.5 mL), respectively. The mixtures were stirred for 10 minutes, concentrated *in vacuo* to a volume of *ca.* 0.2 mL. These solutions were adsorbed on small preparative chromatography plates (basic Al_2O_3, 10 × 10 cm, 0.25 mm), and the elution was performed with CH_2Cl_2–MeCN (3 : 1). One band appeared, which was abraded from the glass surface and suspended in CH_2Cl_2. The resulting suspensions were filtered and concentrated *in vacuo* to afford the desired complexes [Fe(**4**)][Δ-**6**]$_2$, [Fe(**4**)][Λ-**7**]$_2$ or [Fe(**4**)][Δ-**8**]$_2$ as the only eluted salts. Of importance to the present study is the migration of a single chromatographic band during the purification/isolation procedure and the good solubility of the resulting complexes in low polarity solvent.

Computational details

The absolute configuration of the salt [Fe(**4**)][Δ-**8**]$_2$ was determined by comparison of the solution CD spectrum to predictions from time-dependent density functional theory (TDDFT). The energy minimum structure of cation $[Fe(4)]^{2+}$ was obtained using density functional theory (DFT) with the gradient-corrected BP86 functional[25,26] and the resolution-of-the-identity approximation (RI-J).[27] Basis sets were triple-zeta plus polarization (TZVP)[28] for iron and split-valence plus polarization (SVP)[29] for all other elements, along with corresponding auxiliary basis sets.[30] Solvent effects were described using conductor-like solvation model (COSMO).[31]

Results and discussion

Synthesis and characterization of ligands and complexes

Each of the homoditopic ligands **1–5** (Scheme 2) possesses a central naphthalene unit bearing two 4′-substituted-tpy-terminated bis(polyethyleneoxy) metal-binding domains. We have previously reported ligands **1–4** and their reactions to form ruthenamacrocyclic complexes of type $[Ru_nL_n]^{2n+}$ (n = 2 or 3).[12] For these ligands, the optimal method of synthesis varied for each compound. The three strategies that we explored were (i) treatment of 4′-chloro-2,2′:6′,2″-terpyridine (Cltpy) with bis(alcohol)-functionalized naphthalene, (ii) reaction of 4′-hydroxy-2,2′:6′,2″-terpyridine (HOtpy) with a naphthalene containing two electrophilic substituents or (iii) treatment of alcohol-tailed 2,2′:6′,2″-terpyridines with a bis(bromomethyl)-functionalized naphthalene. The synthesis of ligand **5** was most efficiently carried out by the first of these routes (Scheme 3). After chromatographic workup, **5** was isolated as a yellow oil in 14% yield. The ^{1}H and ^{13}C NMR spectra of **5** were fully assigned by using COSY, NOESY, HMQC and HMBC techniques. In the mass spectrum of **5**, the highest mass peak at m/z 887 was assigned to $[M]^+$; the base peak at m/z 250 arose from the fragment $[tpyOH]^+$.

Each of ligands **1–5** was treated with iron(II) chloride in a 1 : 1 molar ratio, under moderately high dilution conditions to encourage the formation of discrete complexes in preference to polymeric species. Each reaction gave a purple, iron(II)-containing product that was isolated as a hexafluorophosphate salt. In each case, only one major component could be chromatographically separated from the reaction mixture. All other products remained as intractable solids on the baseline and were assumed to be metallopolymers. Since our main interest in this work was in the metallocyclic complexes, all of which were formed in reasonable yields, no attempt was made to characterize products that were not separable by conventional chromatographic methods.

The product from the reaction of iron(II) chloride with ligand **1** was characterized as the [2 + 2] metallomacrocyclic complex $[Fe_2(\mathbf{1})_2]^{4+}$. The highest mass peak in the ES mass spectrum appeared at m/z 578, and had the correct isotope distribution for $[M - 3PF_6]^{3+}$. The base peak at m/z 398 was assigned to $[M - 4PF_6]^{4+}$. A comparison of the ^{1}H NMR spectra of ligand **1** and that of the complex formed with iron(II) showed the expected shift of the signal for H^{A6} to lower frequency (Table 1). In addition, the signals for H^{A4} and H^{A5} appear at lower frequency on going from **1** to the complex, and this is evidence for the formation of a macrocyclic product. We have previously observed that the

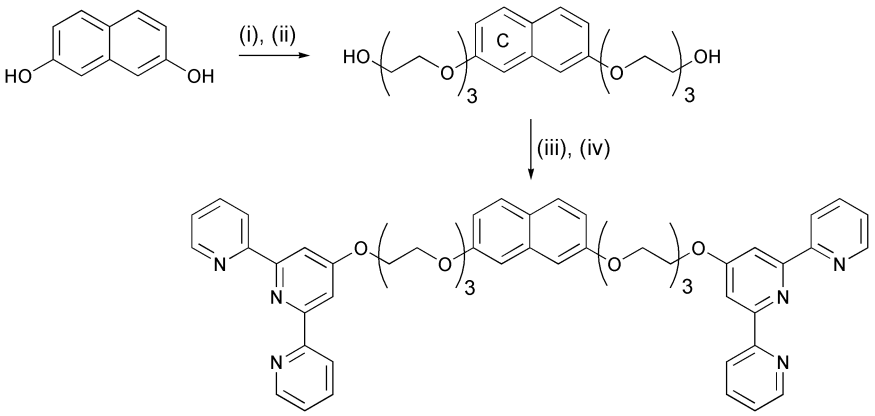

Scheme 3 Synthetic route to ligand **5**: (i) K_2CO_3, acetone, 70 °C, 2 h; (ii) $Cl(CH_2CH_2O)_2CH_2CH_2OH$, 70 °C, 5 days; (iii) KOH, DMSO, 70 °C, 1 h; (iv) Cltpy, 70 °C, 5 days. The ring labelling in the intermediate is used for the NMR spectroscopic assignments (see also Scheme 2).

formation of $[Ru_2(\mathbf{1})_2]^{4+}$ (the cyclic structure of which has been crystallographically confirmed) is accompanied by diagnostic shifts in the signals for H^{A4} and H^{A5} to lower frequencies.[12] The formation of the [2 + 2] product with ligand **1** was expected on the basis of modelling, which indicated that the spacer was too short to allow the [1 + 1] product.

Ligands **2** and **3** possess tpy-terminated polyethyleneoxy-substituents in the 2 and 3-positions of the naphthalene spacer. The ^{1}H NMR spectrum of the purple product of the reaction of **2** with iron(II) chloride showed a single tpy and a single naphthalene environment, indicating the formation of a symmetrical species. A comparison of the ^{1}H NMR spectra of **2** and its iron(II) complex confirmed the changes expected upon coordination and upon the formation of a metallomacrocycle; changes in the chemical shifts for protons H^{B3}, H^{A6}, H^{A4} and H^{A5} (Table 1) were especially diagnostic as noted above. Evidence for the formation of a [3 + 3] metallomacrocycle came from the ES mass spectrum in which a peak at m/z = 383 was assigned to $[M - 6PF_6]^{6+}$; the observed isotope pattern matched that simulated. Complex $[Fe_3(\mathbf{2})_3]^{6+}$ was formed in 38% yield. Increasing the length of the polyethyleneoxy chain on going from **2** to **3** resulted in the preferential formation of a [2 + 2] metallomacrocyclic complex, $[Fe_2(\mathbf{3})_2]^{4+}$. Once again, the signals for protons H^{B3} and H^{A6} (Table 1) were diagnostic probes for coordination of the ligand, while those for H^{A4} and H^{A5} provided evidence for the formation of a metallomacrocycle as opposed to a linear complex.[12] In the electrospray mass spectrum, peaks at m/z = 618 and 427 were assigned to $[M - 3PF_6]^{3+}$ and $[M - 4PF_6]^{4+}$, respectively. The preference for the [2 + 2] ferracycle formation with ligand **3**, but a [3 + 3] ferracycle for ligand **2** arises from the lengthening of the spacer and consequent relief of strain in the lower nuclearity species. Interestingly, we have been able to isolate dinuclear ruthenacycles $[Ru_2(\mathbf{2})_2]^{4+}$ and $[Ru_2(\mathbf{3})_2]^{4+}$, although the former only in 1% yield.[12]

The coordination of iron(II) with ligand **4** or **5** led, in each case, to the unexpected formation of a [1 + 1] macrocycle. This composition was evident from the appearance in the ES mass spectra of peaks arising from $[M - PF_6]^+$ (m/z 999 for $[Fe(\mathbf{4})][PF_6]_2$ and 1087 for $[Fe(\mathbf{5})][PF_6]_2$), and $[M - 2PF_6]^{2+}$ (m/z 471 for $[Fe(\mathbf{5})][PF_6]_2$). However, room temperature (298 K) 500 MHz ^{1}H NMR spectroscopic data indicated that the solution properties (in CD_3CN) of the two complexes differed significantly from one another. The ^{1}H NMR spectrum of $[Fe(\mathbf{5})][PF_6]_2$ exhibited only one set of tpy proton signals that showed that the two terminal rings of each tpy ligand were equivalent (Fig. 1). In contrast, the ^{1}H NMR spectrum of $[Fe(\mathbf{4})][PF_6]_2$ (Fig. 2) exhibited two sets of tpy signals in a 1 : 1 ratio. The desymmetrization of the spectrum could arise from (i) the two tpy ligands being in chemically or magnetically different environments or (ii) each ligand being desymmetrized such that the A and D rings were no longer equivalent.

The key experiment in distinguishing these possibilities lies in the observation of a COSY cross peak between the two

Table 1 ^{1}H NMR chemical shifts for protons in the tpy and naphthalene units of free and coordinated ligands **1** to **5**. All complexes were characterized as $[PF_6]^-$ salts; measurements are at room temperature; solvents for ligands and complexes are $CDCl_3$ and CD_3CN respectively. Ring labelling is given in Schemes 2 and 3

Ligand or cation	H^{A3}	H^{A4}	H^{A5}	H^{A6}	H^{B3}	H^{C1}	H^{C3}	H^{C4}	H^{C5}	H^{C6}
1	8.61	7.84	7.32	8.68	8.07	7.81	7.49	7.81		
2	8.57	7.83	7.30	8.64	8.06	7.28			7.70	7.35
3	8.56	7.80	7.28	8.64	8.02	7.14			7.63	7.28
4	8.60	7.84	7.31	8.67	8.05	7.02	7.02	7.60		
5	8.59	7.83	7.31	8.66	8.04	6.98	6.98	7.58		
$[Fe_2(\mathbf{1})_2]^{4+}$	8.29	7.71	6.87	6.99	8.47	7.72	7.34	7.47		
$[Fe_3(\mathbf{2})_3]^{6+}$	8.35	7.60	6.87	7.12	8.54	7.59			7.88	7.46
$[Fe_2(\mathbf{3})_2]^{4+}$	8.19	7.33	6.65	6.98	8.41	7.35			7.67	7.29
$[Fe(\mathbf{4})]^{2+}$	8.18 H^{A3}	7.31 H^{A4}	6.52 H^{A5}	6.65 H^{A6}	8.82 H^{B3}	4.86	6.85	7.53		
	8.37 H^{D3}	7.84 H^{D4}	7.02 H^{D5}	7.35 H^{D6}	8.41 H^{B5}					
$[Fe(\mathbf{5})]^{2+}$	8.23	7.60	6.87	7.07	8.51	5.44	6.87	7.59		

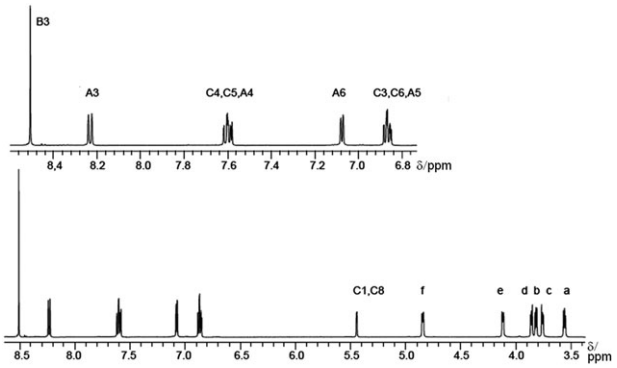

Fig. 1 The ^{1}H NMR spectrum (500 MHz) of [Fe(**5**)][PF_6]$_2$ in CD_3CN solution at room temperature.

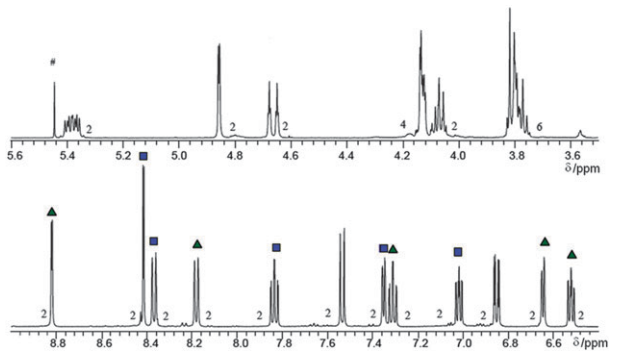

Fig. 2 The ^{1}H NMR spectrum (500 MHz) of [Fe(**4**)][PF_6]$_2$ in CD_3CN solution at room temperature. ($^{\#}$ is residual CH_2Cl_2, the number next to the signal is the relative integral, and the triangles and squares indicate the two sets of tpy proton signals).

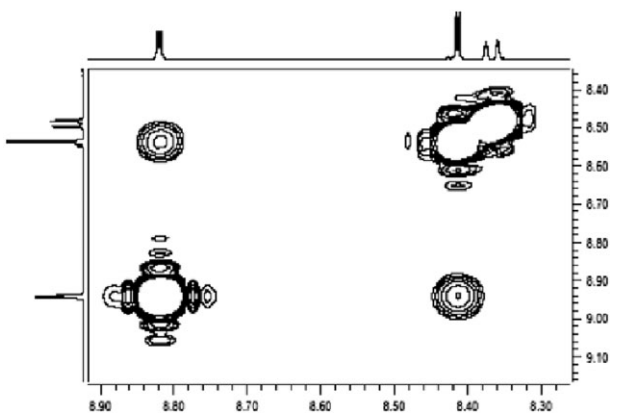

Fig. 3 Part of the ^{1}H–^{1}H COSY spectrum (500 MHz) of [{Fe(**4**)}][PF_6]$_2$ in CD_3CN solution at room temperature showing the coupling of the HB3 and HB5 protons. Chemical shifts in δ/ppm.

doublets observed for the H^{B3} and H^{B5} protons (J = 2.2 Hz, Fig. 3) which can only result in the case of the desymmetrized tpy. The spectrum also showed two sets of signals for methylene groups, and of the three signals assigned to naphthalene protons, one was shifted to unusually low frequency (δ 4.86 ppm). The ^{1}H and ^{13}C NMR spectra of the complexes were assigned by using COSY, NOESY, DEPT, HMQC and HMBC techniques.

A preliminary report of the structure and conformationally locked nature of the [Fe(**4**)]$^{2+}$ cation in [Fe(**4**)][PF_6]$_2$ has already been published.[9] The molecular structure of [Fe(**4**)]$^{2+}$ is shown in Fig. 4 and selected bond distances and angles are given in the caption. We have now determined the single crystal structure of the related complex [Fe(**5**)][PF_6]$_2$·MeCN, suitable crystals being grown from an acetonitrile solution of [Fe(**5**)][PF_6]$_2$. The structure of the [Fe(**5**)]$^{2+}$ ion is shown in Fig. 5. The crystallographic results confirm that both complexes are [1 + 1] metallomacrocycles. In each complex, the naphthalene spacer is positioned between the blades of the two tpy ligands such that it is coplanar with one (although there are no significant π-stacking interactions) and perpendicular to the second (Fig. 4). The naphthalene protons attached to atoms C(27) and C(29) in [Fe(**4**)]$^{2+}$ point directly at the π-cloud of the pyridine ring containing atom N(4). The distances between the atoms H(271) and H(291) and the least squares plane of this ring are 3.23 and 3.63 Å, respectively, and between H(271) and H(291) and the ring-centroid are 3.69 and 3.71 Å, respectively. This observation is consistent with the low frequency (δ 4.86 ppm) of the ^{1}H NMR signal assigned to these protons (see above), which arises from them lying in the anisotropic shielding region above the pyridine ring. Similarly, in [Fe(**5**)]$^{2+}$, the naphthalene protons attached to atoms C(44) and C(46) point towards the pyridine ring containing atom N(6). However, in the solid state, only one hydrogen atom is positioned directly over the ring; distances between atoms H(441) and H(461) and the least squares plane of ring containing N(6) are 3.20 and 2.57 Å, respectively, and between H(441) and H(461) and the ring-centroid are 3.40 and 4.33 Å, respectively. In the solid state, the arrangement of the polyethyleneoxy chain with respect to the {Fe(tpy)$_2$} unit renders

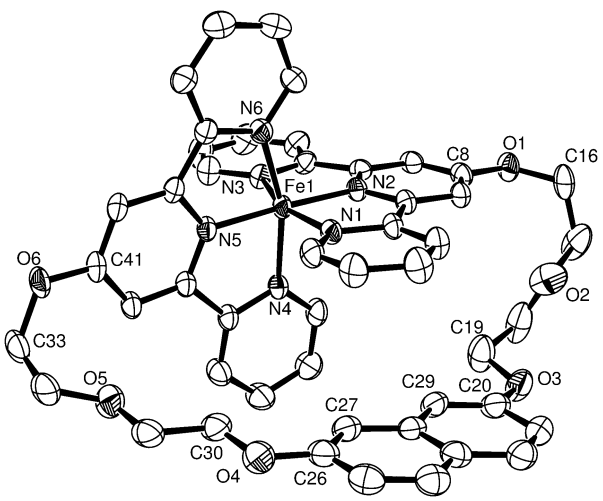

Fig. 4 Structure of the [Fe(**4**)]$^{2+}$ cation in [Fe(**4**)][PF_6]$_2$; hydrogen atoms are omitted. Ellipsoids are drawn at 50% probability. Selected bond distances and angles: Fe(1)–N(1) = 1.962(3), Fe(1)–N(2) = 1.876(3), Fe(1)–N(3) = 1.970(3), Fe(1)–N(4) = 1.970(3), Fe(1)–N(5) = 1.874(3), Fe(1)–N(6) = 1.961(3), O(1)–C(8) = 1.346(4), O(3)–C(20) = 1.366(5), O(4)–C(26) = 1.361(5), O(6)–C(41) = 1.344(4) Å; N(1)–Fe(1)–N(2) = 80.89(12), N(2)–Fe(1)–N(3) = 81.04(13), N(4)–Fe(1)–N(5) = 80.90(12), N(5)–Fe(1)–N(6) = 81.01(13), C(8)–O(1)–C(16) = 121.8(3), C(19)–O(3)–C(20) = 117.3(3), C(26)–O(4)–C(30) = 117.4(3), C(33)–O(6)–C(41) = 120.5(3)°.

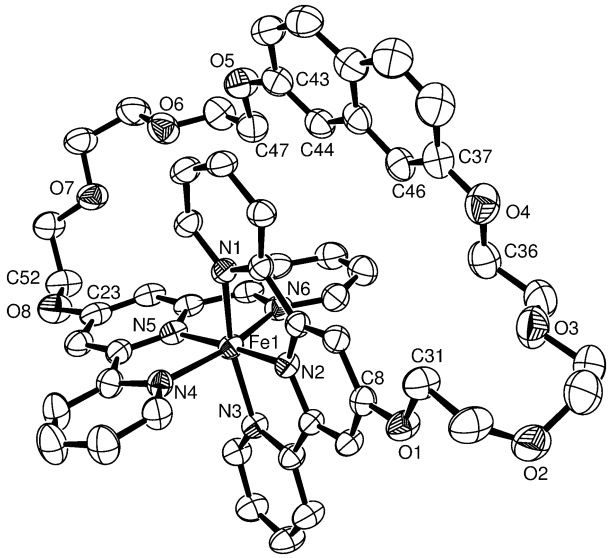

Fig. 5 Structure of the $[Fe(\mathbf{5})]^{2+}$ cation in $[Fe(\mathbf{5})][PF_6]_2{\cdot}CH_3CN$. Ellipsoids are drawn at 50% probability. Selected bond distances and angles: Fe(1)–N(1) = 1.979(2), Fe(1)–N(2) = 1.881(2), Fe(1)–N(3) = 1.971(2), Fe(1)–N(4) = 1.980(2), Fe(1)–N(5) = 1.898(2), Fe(1)–N(6) = 1.968(2), C(8)–O(1) = 1.343(3), C(31)–O(1) = 1.447(3), C(23)–O(8) = 1.352(4), C(52)–O(8) = 1.437(4), C(37)–O(4) = 1.368(4), C(36)–O(4) = 1.429(4), C(43)–O(5) = 1.367(4), C(47)–O(5) = 1.430(4) Å; N(1)–Fe(1)–N(2) = 80.70(9), N(2)–Fe(1)–N(3) = 81.15(9), N(4)–Fe(1)–N(5) = 80.71(10), N(5)–Fe(1)–N(6) = 80.54(10), C(31)–O(1)–C(8) = 118.5(2), C(32)–O(2)–C(33) = 115.5(3), C(34)–O(3)–C(35) = 112.6(3), C(36)–O(4)–C(37) = 117.3(3), C(47)–O(5)–C(43) = 117.2(3), C(49)–O(6)–C(48) = 110.9(3), C(51)–O(7)–C(50) = 113.2(3), C(52)–O(8)–C(23) = 122.2(3)°.

each cation chiral (Fig. 6), although each crystallizes as a racemate. The solution data described above are consistent with $[Fe(\mathbf{4})]^{2+}$ retaining the structure that is present in the solid state, *i.e.* the metallocycle is conformationally locked. In contrast, the polyethyleneoxy chain in $[Fe(\mathbf{5})]^{2+}$ is long enough to allow a skipping rope type of motion around the $\{Fe(tpy)_2\}$ unit such that there is no distinction between "inner" and "outer" pyridine rings on the 500 MHz ^{1}H NMR time scale at room temperature. The shielding of the H^{C1} protons in $[Fe(\mathbf{5})][PF_6]_2$ (δ 5.44) is evidence that the time-averaged structure involves these protons lying in the shielding region above the pyridine at least some of the time.

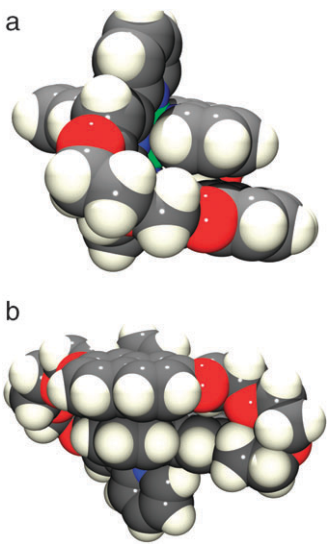

Fig. 6 Space filling diagrams of (a) $[Fe(\mathbf{4})]^{2+}$ and (b) $[Fe(\mathbf{5})]^{2+}$ illustrating the relative orientation of the naphthalene unit with respect to one of the tpy ligands.

A variable temperature proton NMR experiment (500 MHz, 180–298 K) on $[Fe(\mathbf{5})][PF_6]_2$ in CD_2Cl_2 solution was made to investigate possible locking of the naphthalene ring as in the $[Fe(\mathbf{4})][PF_6]_2$. However, there is no evidence for splitting into two sets of signals as in $[Fe(\mathbf{5})][PF_6]_2$, even when the temperature was lowered to 180 K. However, the signals for $H^{C1,\ C8}$, H^{A3} and H^{A4} started to coalesce at around 190 K but those for $H^{N4,\ N6}$ and H^{A6} remained relatively sharp. This gives some information about the movement of the naphthalene ring. It seems that when the naphthalene ring is rotating around the $[Fe(tpy)_2]^{2+}$ unit, the $H^{N1,\ N8}$ protons remain close to the H^{A3} and H^{A4} protons.

An aside on the origin of chirality in $[Fe(4)]^{2+}$ and $[Fe(5)]^{2+}$

The cartoon representation of the enantiomers of the chiral cations presented at the top of Fig. 7 does not sufficiently clarify the origin of the effect. At a global level, the phenomenon is an example of *atropisomerism* arising from the restricted rotation of the linker on the NMR time scale, a view confirmed by the lower barrier (see later) in the complex with the longer chain $[Fe(\mathbf{5})]^{2+}$. Two descriptions of the chirality appear possible. A first possibility would be to associate the stereochemistry with the metal centre and to view the "locked" conformation as a special case of *spiro* chirality with "asymmetric" tpy ligands. The asymmetry would be defined by giving the highest priority to the rings of the terpy ligands closer spatially to the linker. A second and favored description is of *axial chirality*. As mentioned, the core of complexes $[Fe(\mathbf{4})]^{2+}$ and $[Fe(\mathbf{5})]^{2+}$ possesses a framework of D_{2d} symmetry—a symmetry typically involved with allenes, alkylidenecycloalkanes and biphenyls. With proper non-symmetrical substitution at both ends, the *long axis* of these frameworks becomes a *chiral axis*. It is the case with complexes $[Fe(\mathbf{4})]^{2+}$ and $[Fe(\mathbf{5})]^{2+}$ for which the $O_{4'}$–$N_{central}$–Fe–$N_{central}$–$O_{4'}$ axis is *chiral* due to the non-symmetrical positioning of the linker up/down or left/right to the tpy ligands. The asymmetry is defined by the orientation of the linker and the highest priority is given to the quadrants that contain the linker. The *aR* and *aS* enantiomers are displayed in Fig. 7 (bottom). Alternatively, molecules with chiral axes may be viewed as helices and these enantiomers can be viewed as molecules of *M* and *P* configuration, respectively.

Investigations into the solution behaviour of $[Fe(4)]^{2+}$

Chiral mononuclear divalent tris(diimine) or bis(triimine) complexes of first row transition metals are notoriously known for their high chemical but low configurational stability. The Δ and Λ enantiomers can be sometimes isolated in good enantiomeric purity through efficient resolution procedures.[32,33] However, once dissolved, these derivatives racemize rapidly when no other source of chiral information is present on the ligands[34–36] or in the reaction medium.[37–40] The ease of synthesis of $[Fe(\mathbf{4})]^{2+}$ and the rapidity of its formation led us to imagine a possibly

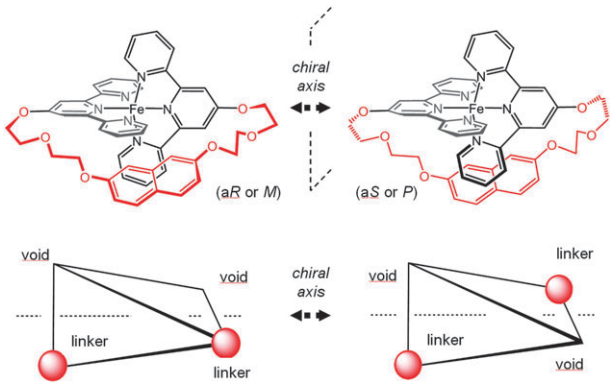

Fig. 7 The two enantiomers of $[Fe(\mathbf{4})]^{2+}$ and a schematic representation of their *axial* (*helical*) *chirality*.

high chemical stability for compound $[Fe(\mathbf{4})][PF_6]_2$. It was then debatable whether it would also mean an increased configurational stability; the *aR* and *aS* enantiomers being possibly, although unlikely, inert and separable from each other.

Previously, hexacoordinated phosphorus anions TRISPHAT **6**,[16,41] SUGARPHAT **7**[18,19] and BINPHAT **8**[17] have been shown to be general NMR chiral solvating, resolving and asymmetry-inducing reagents for chiral cationic species.[42,43] When associated with configurationally stable cations, they behave as general NMR chiral solvating and resolving agents.[44–49] When associated with configurationally *labile* cations, supramolecular diastereoselective interactions can occur and one diastereomeric ion pair can become predominant in solution; the occurrence of such behavior (*Pfeiffer* effect[28,50–59]) being a good probe for the lack of configurational stability of the cation.[53,57–60] For this reason, dication $[Fe(\mathbf{4})]^{2+}$ was studied in the presence of hexacoordinated phosphorus anions TRISPHAT, SUGARPHAT and BINPHAT. Salts $[Fe(\mathbf{4})][\Delta\text{-}\mathbf{6}]_2$, $[Fe(\mathbf{4})][\Lambda\text{-}\mathbf{7}]_2$ and $[Fe(\mathbf{4})][\Delta\text{-}\mathbf{8}]_2$ were prepared according to a literature procedure,[34] and studied by ^{1}H NMR spectroscopy.

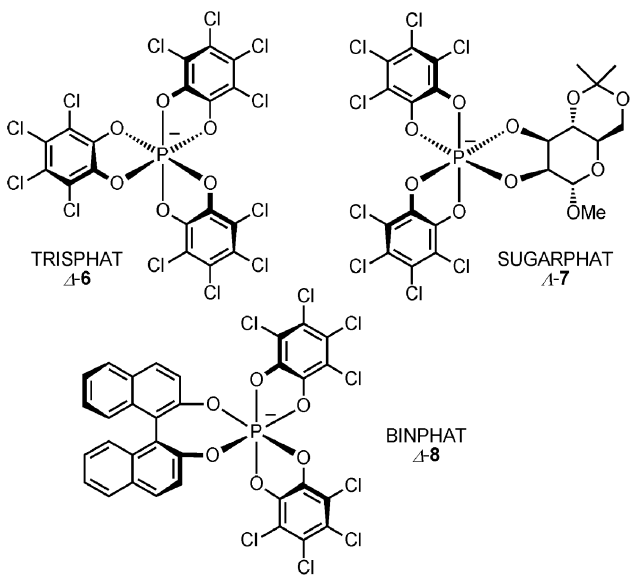

As expected, all anions **6**, **7** and **8** behaved as NMR chiral solvating agents in CD_2Cl_2 for complex Fe(**4**). However, and interestingly, a very different response in the NMR spectra was obtained for the cation in the presence of the different anions (Fig. 8, δ 9.0–7.9 ppm). For $[Fe(\mathbf{4})][\Delta\text{-}\mathbf{6}]_2$, the largest induced separation of the NMR signals ($\Delta\delta$) was observed for the proton in position C3 of the tpy ring (0.03 ppm), the other protons being either unchanged or barely split (H^{B3} $\Delta\delta$ 0.008 ppm). The ratio between the two diastereomeric ion pairs was 1 : 1, as it could be expected for a racemic mixture of cations $[Fe(\mathbf{4})]^{2+}$. For $[Fe(\mathbf{4})][\Lambda\text{-}\mathbf{7}]_2$, the largest $\Delta\delta$ value was measured this time for H^{A3} and H^{B3} of the tpy rings (0.03 ppm); protons H^{C3} (and H^{B5} again) remaining unsplit. As for salt $[Fe(\mathbf{4})][\Delta\text{-}\mathbf{6}]_2$, a 1 : 1 ratio between the two diastereomeric ion pairs was measured. Finally, salt $[Fe(\mathbf{4})][\Delta\text{-}\mathbf{8}]_2$ was analyzed. Due to overlap with the signals of BINPHAT, most of the aromatic protons of $[Fe(\mathbf{4})]^{2+}$ outside the δ 9.0–7.9 ppm window could not be monitored. Nevertheless, even with the short NMR windows available, a completely different and interesting situation was observed. Proton H^{B5}, which so far had not been influenced by the chiral counterions, was nicely separated into two doublet signals ($\Delta\delta$ 0.08 ppm). Overall, as it is most often the case with organic cations, BINPHAT was more effective as a chiral NMR solvating agent than TRISPHAT and SUGARPHAT. Furthermore and in sharp contrast to the situation in the other salts, integration of the separated signals indicated an imbalance in the diastereomeric population and the predominance of one atropisomeric cation over the other (diastereomeric ratio d.r. 1.5 : 1, diastereomeric excess d.e. 20%, Fig. 8, spectrum d).

Two hypotheses were then considered to explain the above-described results: (i) a configurational stability for ion Fe(**4**) and a partial resolution of its enantiomers during the ion pair metathesis of the hexafluorophosphate to the BINPHAT salts or (ii) a configurational lability and the occurrence of a supramolecular stereocontrol from anion *Λ*-BINPHAT over the geometry of cations Fe(**4**); one of the diastereomeric ion pairs, $[(aS)\text{-}Fe(\mathbf{4})][\Delta\text{-}\mathbf{8}]_2$ or $[(aR)\text{-}Fe(\mathbf{4})][\Delta\text{-}\mathbf{8}]_2$, being thermodynamically more stable and thus preferred in solution.

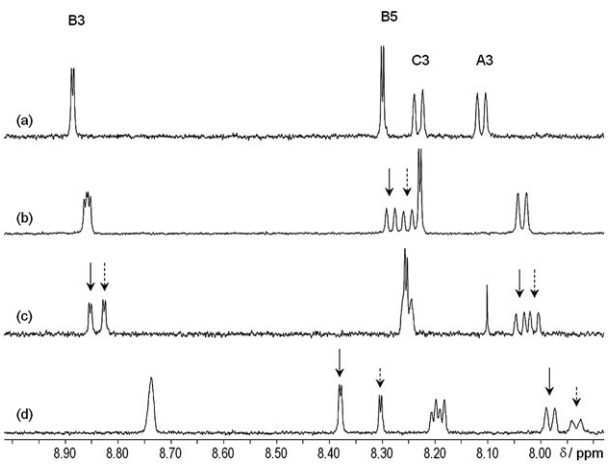

Fig. 8 The ^{1}H NMR spectra (500 MHz, CD_2Cl_2, 293 K, δ 9.0–7.9 ppm) of the salts of $[Fe(\mathbf{4})]^{2+}$. Counter ions: (a) $[PF_6]^-$, (b) *Δ*-**6**, (c) *Λ*-**7** and (d) *Δ*-**8**; plain and dashed arrows indicating diastereomeric signals.

To discriminate between these two hypotheses, a series of studies was performed in solvent combinations of various polarity. It is well known that stereoselective recognition among chiral ions regularly is only achieved in low polarity solvents.[61,62] In high polarity media, poor chiral discriminations occur as a result of weaker electrostatic interactions and solvent competition.[63] Thus, with salts made of configurationally labile cations, the maximum diastereoselectivity is achieved in low polar solvents and varies with modifications of the solvent polarity. If the cation is configurationally stable, ratios between diastereomers are, on the contrary, solvent-independent.

Chloroform ($CDCl_3$) solutions of [Fe(**4**)][*Δ*-**8**]$_2$ were prepared with some content of polar DMSO-d_6 (2%, 5%, 10% and 20%). The spectra are reported in Fig. 9. Clearly, the BINPHAT anion behaves as an NMR chiral solvating agent in all cases (*i.e.* for proton H^{B5}) and different values are obtained for the diastereomeric ratios in the different solvent combinations (as shown by the various integration values). The diastereoselectivity is best in 2% DMSO–$CDCl_3$ (d.e. 60%, δ 0.14 ppm for H^{B5}) and decreases gradually from 5% (d.e. 50%, δ 0.14 ppm) to 10% (d.e. 42%, δ 0.09 ppm) and then 20% (d.e. 17%, δ 0.03 ppm), that is going from the less polar to the more polar solvent conditions.

The occurrence of the asymmetric ion pairing was then ascertained by circular dichroism (CD) ($\sim 10^{-4}$ M range). The CD spectra of solutions of complex [Fe(**4**)][*Δ*-**8**]$_2$ revealed positive and negative Cotton effects around 611 and 561 nm, respectively (see Fig. 10). The enantiomeric complex [Fe(**4**)][*Δ*-**8**]$_2$ was then prepared and displayed, as expected, negative and positive Cotton effects around 611 and 561 nm, respectively.

Electronic excitation energies and rotatory strengths of $[Fe(\mathbf{4})]^{2+}$ were computed from TDDFT linear response at

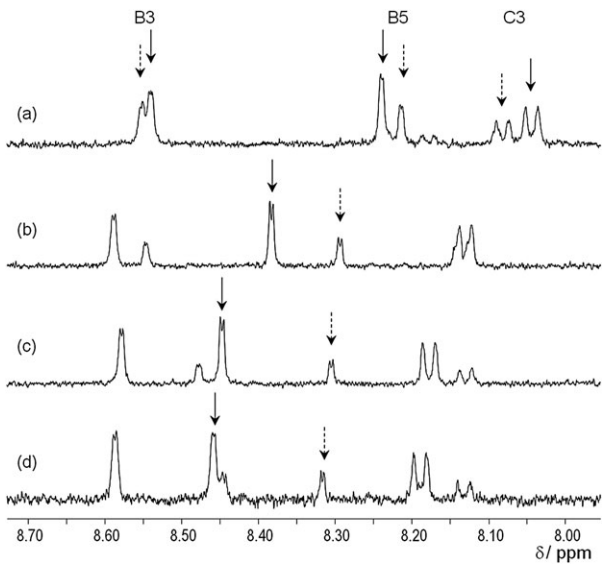

Fig. 9 ^{1}H NMR spectra (400 MHz, parts, 293 K) of [Fe(**4**)][*Δ*-**8**]$_2$ in different % of DMSO-d_6 in $CDCl_3$ and subsequent diastereoselectivity: (a) 20% DMSO (d.e. 17%); (b) 10% DMSO (d.e. 42%); (c) 5% DMSO (d.e. 50%) and (d) 2% DMSO (d.e. 60%); plain and dashed arrows indicating signals of the major and minor diastereomers, respectively.

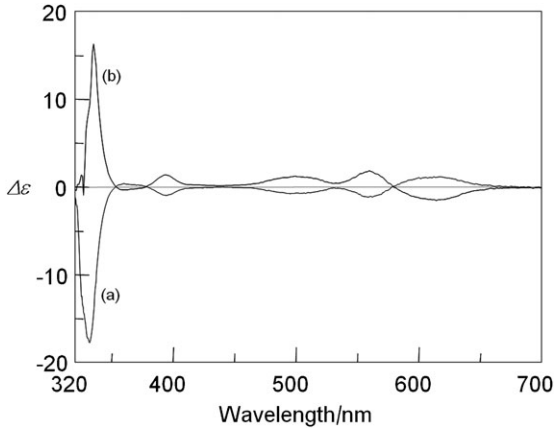

Fig. 10 Induced CD spectra of salts (a) [Fe(**4**)][*Δ*-**8**]$_2$ and (b) [Fe(**4**)][*Λ*-**8**]$_2$, 1% DMSO in chloroform, 1.09×10^{-4} M, 20 °C.

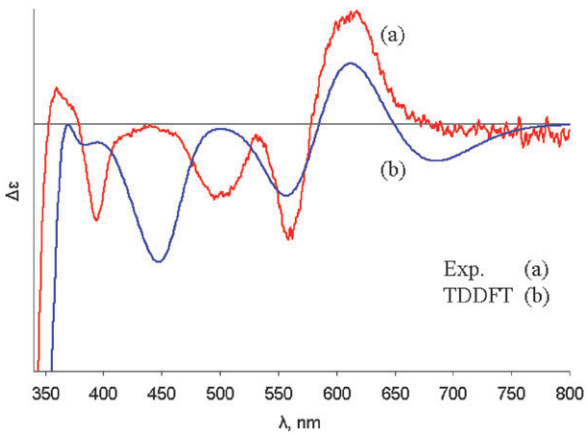

Fig. 11 Comparison of (a) experimental (10^{-4} mol l^{-1} in $CHCl_3$) and (b) computed CD spectra of [Fe(**4**)][*Δ*-**8**]$_2$.

the same level of theory as described in the experimental section.[64,65] An experimental CD spectrum was simulated by Gaussian line broadening using an empirical line width of 0.1 eV. All calculations were performed with the quantum chemistry package Turbomole.[66] The CD spectrum of $[Fe(\mathbf{4})]^{2+}$ was simulated using TDDFT calculations and experimental and computed CD spectra are shown in Fig. 11. Very good agreement is found between the theory and experiment, in particular, the positive and negative Cotton effects at 611 nm and 561 nm, respectively, are well reproduced. The agreement at lower wavelengths is less satisfactory, which is expected due to a large number of electronic transitions of opposite sign which partially cancel each other. The TDDFT results are thus expected to be most reliable at low excitation energies, *viz.* at the red edge of the CD spectrum, in accord with our findings. However, even the low-energy CD bands consist of several close-lying electronic transitions. The positive Cotton band at 611 nm is mainly due to metal-to-ligand excitations, whereas the negative Cotton band at 561 nm involves excitations from the naphthalene unit. The chiral induction due to the dissymmetric spacer group is well described by TDDFT and allows an unequivocal assignment of the *aR* absolute configuration to the $[Fe(\mathbf{4})]^{2+}$ cation in Fe(**4**)][*Δ*-**8**]$_2$. Accordingly, the red and blue spectra in

Fig. 10 of complexes [Fe(**4**)][*Λ*-**8**]$_2$ and [Fe(**4**)][*Λ*-**8**]$_2$ are assigned to the *aR* and *aS* absolute configurations of the cations, respectively.

Conclusions

In conclusion, we have shown that ditopic bis(2,2′:6′,2″-terpyridine) ligands give rise to conformationally restricted complexes with iron(II) centres. The 1 : 1 cations are chiral and diastereoisomeric enrichments may be achieved using the Pfeiffer effect. The absolute configuration of the cations in the diastereomeric ion pairs obtained through the Pfeiffer effect has been calculated using TDDFT methods.

Acknowledgements

We thank the Swiss National Science Foundation, the Swiss nanoscience Institute, the University of Basel, the State Secretariat for Education and Research and the University of Geneva for financial support. The calculations were performed at the University of Karlsruhe. D. R. thanks Filipp Furche for support and helpful discussions.

References

1 G. B. Kauffman, *Coordination chemistry: a century of progress*, American Chemical Society, Washington, DC, 1994.
2 A. von Zelewsky, *Stereochemistry of coordination compounds*, Wiley, Chichester, England, New York, 1996.
3 A. E. Martell and M. Calvin, *Chemistry of the metal chelate compounds*, Prentice-Hall, New York, 1952.
4 H. Hofmeier and U. S. Schubert, *Chem. Soc. Rev.*, 2004, **33**, 373.
5 U. Schubert, H. Hofmeier and G. R. Newkome, *Modern Terpyridine Chemistry*, Wiley-VCH, Weinheim, 2006.
6 E. C. Constable, *Chem. Soc. Rev.*, 2007, **36**, 246.
7 E. C. Constable, *Adv. Inorg. Chem.*, 1987, **30**, 69.
8 C. B. Smith, E. C. Constable, C. E. Housecroft and B. M. Kariuki, *Chem. Commun.*, 2002, 2068.
9 H. S. Chow, E. C. Constable, C. E. Housecroft and M. Neuburger, *Dalton Trans.*, 2003, 4568.
10 E. C. Constable, C. E. Housecroft and C. B. Smith, *Inorg. Chem. Commun.*, 2003, **6**, 1011.
11 E. C. Constable, C. E. Housecroft, M. Neuburger, S. Schaffner and C. B. Smith, *Dalton Trans.*, 2005, 2259.
12 H. S. Chow, E. C. Constable, C. E. Housecroft, M. Neuburger and S. Schaffner, *Polyhedron*, 2006, **25**, 1831.
13 E. C. Constable, K. Harris, C. E. Housecroft, M. Neuburger and S. Schaffner, *Chem. Commun.*, 2008, 5360.
14 E. L. Eliel, S. H. Wilen and L. N. Mander, *Stereochemistry of organic compounds*, Wiley, New York, 1994.
15 E. C. Constable and M. D. Ward, *J. Chem. Soc., Dalton Trans.*, 1990, 1405.
16 J. Lacour, C. Ginglinger, C. Grivet and G. Bernardinelli, *Angew. Chem., Int. Ed. Engl.*, 1997, **36**, 608.
17 J. Lacour, A. Londez, C. Goujon-Ginglinger, V. Buß and G. Bernardinelli, *Org. Lett.*, 2000, **2**, 4185.
18 C. Pérollier, S. Constant, J. J. Jodry, G. Bernardinelli and J. Lacour, *Chem. Commun.*, 2003, 2014.
19 C. Pérollier, G. Bernardinelli and J. Lacour, *Chirality*, 2008, **20**, 313.
20 *COLLECT Software*, Nonius BV, 1997–2001.
21 A. Altomare, G. Cascarano, C. Giacovazzo, A. Guagliardi, M. C. Burla, G. Polidori and M. Camalli, *J. Appl. Crystallogr.*, 1994, **27**, 435.
22 Z. Otwinowski and W. Minor, *Methods Enzymol.*, 1997, **276**, 307.
23 P. W. Betteridge, J. R. Carruthers, R. I. Cooper, K. Prout and D. J. Watkin, *J. Appl. Crystallogr.*, 2003, **36**, 1487.
24 L. Farrugia, *J. Appl. Crystallogr.*, 1997, **30**, 565.
25 A. D. Becke, *Phys. Rev. A*, 1988, **38**, 3098.
26 J. P. Perdew, *Phys. Rev. B: Condens. Matter Mater. Phys.*, 1986, **33**, 8822.
27 K. Eichkorn, O. Treutler, H. Öhm, M. Häser and R. Ahlrichs, *Chem. Phys. Lett.*, 1995, **242**, 652.
28 A. Schäfer, C. Huber and R. Ahlrichs, *J. Chem. Phys.*, 1994, **100**, 5829.
29 A. Schäfer, H. Horn and R. Ahlrichs, *J. Chem. Phys.*, 1992, **97**, 2571.
30 K. Eichkorn, F. Weigend, O. Treutler and R. Ahlrichs, *Theor. Chem. Acc.*, 1997, **97**, 119.
31 A. Klamt and G. Schüürmann, *J. Chem. Soc., Perkin Trans. 2*, 1993, 799.
32 F. P. Dwyer and E. C. Gyarfas, *J. Proc. R. Soc. N. S. W.*, 1950, **83**, 263.
33 A. Yamagishi and M. Soma, *J. Chem. Soc., Chem. Commun.*, 1981, 539.
34 J.-L. Pierre, *Coord. Chem. Rev.*, 1998, **178–180**, 1183.
35 A. von Zelewsky, *Coord. Chem. Rev.*, 1999, **190–192**, 811.
36 A. von Zelewsky and O. Mamula, *J. Chem. Soc., Dalton Trans.*, 2000, 219.
37 S. Kirschner, N. Ahmad, C. Munir and R. J. Pollock, *Pure Appl. Chem.*, 1979, **51**, 913.
38 S. Kirschner and I. Bakkar, *Coord. Chem. Rev.*, 1982, **43**, 325.
39 S. Kirschner, T. Gish and U. Freeman, Jr, *ACS Symp. Ser.*, 1994, **565**, 303.
40 K. Nakashima and S. Shinkai, *Chem. Lett.*, 1994, 1267.
41 F. Favarger, C. Goujon-Ginglinger, D. Monchaud and J. Lacour, *J. Org. Chem.*, 2004, **69**, 8521.
42 J. Lacour and R. Frantz, *Org. Biomol. Chem.*, 2005, **3**, 15.
43 J. Lacour and D. Linder, *Chem. Rec.*, 2007, **7**, 275.
44 C. Ginglinger, D. Jeannerat, J. Lacour, S. Jugé and J. Uziel, *Tetrahedron Lett.*, 1998, **39**, 7495.
45 J. Lacour, S. Torche-Haldimann, J. J. Jodry, C. Ginglinger and F. Favarger, *Chem. Commun.*, 1998, 1733.
46 J. Lacour, C. Goujon-Ginglinger, S. Torche-Haldimann and J. J. Jodry, *Angew. Chem., Int. Ed.*, 2000, **39**, 3695.
47 J. Lacour, L. Vial and C. Herse, *Org. Lett.*, 2002, **4**, 1351.
48 D. Monchaud, J. J. Jodry, D. Pomeranc, V. Heitz, J.-C. Chambron, J.-P. Sauvage and J. Lacour, *Angew. Chem., Int. Ed.*, 2002, **41**, 2317.
49 C. Herse, D. Bas, F. C. Krebs, T. Bürgi, J. Weber, T. Wesolowski, B. W. Laursen and J. Lacour, *Angew. Chem., Int. Ed.*, 2003, **42**, 3162.
50 P. Pfeiffer and K. Quehl, *Ber. Dtsch. Chem. Ges.*, 1931, **64**, 2667.
51 B. Norden and F. Tjerneld, *FEBS Lett.*, 1976, **67**, 368.
52 M. M. Green, C. Khatri and N. C. Peterson, *J. Am. Chem. Soc.*, 1993, **115**, 4941.
53 J. Lacour, J. J. Jodry and D. Monchaud, *Chem. Commun.*, 2001, 2302.
54 R. M. Yeh, M. Ziegler, D. W. Johnson, A. J. Terpin and K. N. Raymond, *Inorg. Chem.*, 2001, **40**, 2216.
55 C. Bonnot, J.-C. Chambron and E. Espinosa, *J. Am. Chem. Soc.*, 2004, **126**, 11412.
56 R. M. Yeh and K. N. Raymond, *Inorg. Chem.*, 2006, **45**, 1130.
57 J. Lacour, J. J. Jodry, C. Ginglinger and S. Torche-Haldimann, *Angew. Chem., Int. Ed.*, 1998, **37**, 2379.
58 L. Vial and J. Lacour, *Org. Lett.*, 2002, **4**, 3939.
59 V. Desvergnes-Breuil, V. Hebbe, C. Dietrich-Buchecker, J.-P. Sauvage and J. Lacour, *Inorg. Chem.*, 2003, **42**, 255.
60 J. J. Jodry, R. Frantz and J. Lacour, *Inorg. Chem.*, 2004, **43**, 3329.
61 V. Hebbe-Viton, V. Desvergnes, J. J. Jodry, C. Dietrich-Buchecker, J.-P. Sauvage and J. Lacour, *Dalton Trans.*, 2006, 2058.
62 S. D. Bergman, R. Frantz, D. Gut, M. Kol and J. Lacour, *Chem. Commun.*, 2006, 850.
63 E. Martínez-Viviente, P. S. Pregosin, L. Vial, C. Herse and J. Lacour, *Chem.–Eur. J.*, 2004, **10**, 2912.
64 R. Bauernschmitt and R. Ahlrichs, *Chem. Phys. Lett.*, 1996, **256**, 454.
65 R. Bauernschmitt and R. Ahlrichs, *Chem. Phys. Lett.*, 1997, **264**, 573.
66 R. Ahlrichs, M. Bär, M. Häser, H. Horn and C. Kölmel, *Chem. Phys. Lett.*, 1989, **162**, 165, for the current version see http://www.turbomole.com.